

Connecting physics to systems with modular spin-circuits

Kemal Selcuk,¹ Saleh Bunaiyan,^{1,2} Nihal Sanjay Singh,¹ Shehrin Sayed,³ Samiran Ganguly,⁴ Giovanni Finocchio,⁵ Supriyo Datta,⁶ and Kerem Y. Camsari¹

¹*Department of Electrical and Computer Engineering, University of California, Santa Barbara, CA, 93106, USA*

²*Electrical Engineering Department, King Fahd University of Petroleum & Minerals (KFUPM), Dhahran 31261, Saudi Arabia*

³*TDK Headway Technologies, Inc., Milpitas, CA, 95035, USA*

⁴*Department of Electrical and Computer Engineering, Virginia Commonwealth University, Richmond, VA 23284, USA*

⁵*Department of Mathematical and Computer Sciences, Physical Sciences and Earth Sciences, University of Messina, Messina, Italy*

⁶*Elmore Family School of Electrical and Computer Engineering, Purdue University, West Lafayette, Indiana, 47907, USA*

An emerging paradigm in modern electronics is that of CMOS + X requiring the integration of standard CMOS technology with novel materials and technologies denoted by X. In this context, a crucial challenge is to develop accurate circuit models for X that are compatible with standard models for CMOS-based circuits and systems. In this perspective we present physics-based, experimentally benchmarked modular circuit models that can be used to evaluate a class of CMOS + X systems, where X denotes magnetic and spintronic materials and phenomena. This class of materials is particularly challenging because they go beyond conventional charge-based phenomena and involve the spin degree of freedom which involves non-trivial quantum effects. Starting from density matrices – the central quantity in quantum transport – using well-defined approximations, it is possible to obtain spin-circuits that generalize ordinary circuit theory to 4-component currents and voltages (1 for charge and 3 for spin). With step-by-step examples that progressively go higher in the computing stack, we illustrate how the spin-circuit approach can be used to start from the physics of magnetism and spintronics to enable accurate system-level evaluations. We believe the core approach can be extended to include other quantum degrees of freedom like valley and pseudospins starting from corresponding density matrices.

I. INTRODUCTION

The rise of Artificial Intelligence with its skyrocketing computing needs coincided with the stagnation of Moore’s Law. This clash has been driving the development of domain-specific hardware¹ and architectures with a rich variety of heterogeneous systems for computing, memory and sensing applications. In this new era, rapid and accurate tools for evaluating the potential of emerging materials, physical phenomena, and device concepts has become a crucial need. Such tools will have an impact not only in moving forward well-established computational schemes but also in opening new directions in unconventional computing paradigms².

In this perspective, we describe a physics-based circuit approach that covers a wide range of phenomena in spintronics and magnetism using a generalized circuit theory. We show how circuit “modules” derived out of microscopic theory and phenomenological models can accurately model spin transport while accounting for magnetization dynamics.

Combining phenomenology and microscopic theory, the spin-circuit approach for spintronics has been used to model non-local spin-valves, channels with high-spin orbit coupling such as semiconductor channels with Rashba interactions, heavy metals and topological insulators, transport in ferromagnetic insulators, ferromagnet-normal metal interfaces, spin-pumping phenomena, magnetic tunnel junctions, voltage controlled magnetic anisotropy, finite temperature magnetization dynamics and others. A web page with open-source models along with open-source SPICE codes catalogue these results³.

The key strength of the approach is not just about modeling phenomena, but more about its ability to *combine* the modules to design *new* circuits and structures. For example, given interface, bulk magnet, magnetization dynamics, and spin-orbit channel modules, complicated new devices can be constructed

and studied (see, for example, Ref’s.^{4,5}). Real-time simulation of nanomagnet dynamics coupled with transport modules allows accurate transient simulations from which device characteristics can be obtained. Powerful tools and analysis options of mature circuit simulators greatly ease a wide range of measurements for AC, DC, transient and noise analysis.

Another distinguishing aspect of spin-circuits compared to powerful alternatives to model spintronic phenomena^{6,7} is how new devices and phenomena can be seamlessly integrated with state-of-the-art complementary metal oxide semiconductor (CMOS) transistor models. This combination allows fast, accurate and informative evaluation of CMOS + X platforms (where X can be any emerging CMOS-compatible technology such as spintronics, ferroelectrics, photonics, etc.) using efficient circuit simulators (e.g., SPICE and its variants).

The spin-circuit approach evolved out of a 2-component model involving collinear spins⁸ which is relatively intuitive. It is as if there are two species of electrons, up and down. The charge current is the sum of up and down currents, while the spin current is given by their difference.

Less intuitive is the 4-component model with noncollinear components, 1 for charge and 3 for spin (see, for example,^{9,10} and references therein). The 4-component model is not based on four species of electrons. Rather, it is based on two components with complex amplitudes $\{u\ v\}$ that embody subtle quantum physics. For example, $\{1\ 0\}$ represents $+z$ spin, $\{0\ 1\}$ represents $-z$ spin, while a superposition of the two $\{1\ 1\}$ represents $+x$ spin. This can lead to quite non-intuitive results, like a flux of $+x$ spins getting converted into $+z$ spins by a shunt path that pulls out $-z$ spins¹¹.

Even such non-intuitive effects are accurately captured by the 4-component model whose components represent measurable quantities given by bilinear products of u and v ; the charge component is given by $uu^* + vv^*$ while the three components of spin are given by $uu^* - vv^*$, $\text{Re}(uv^*)$ and

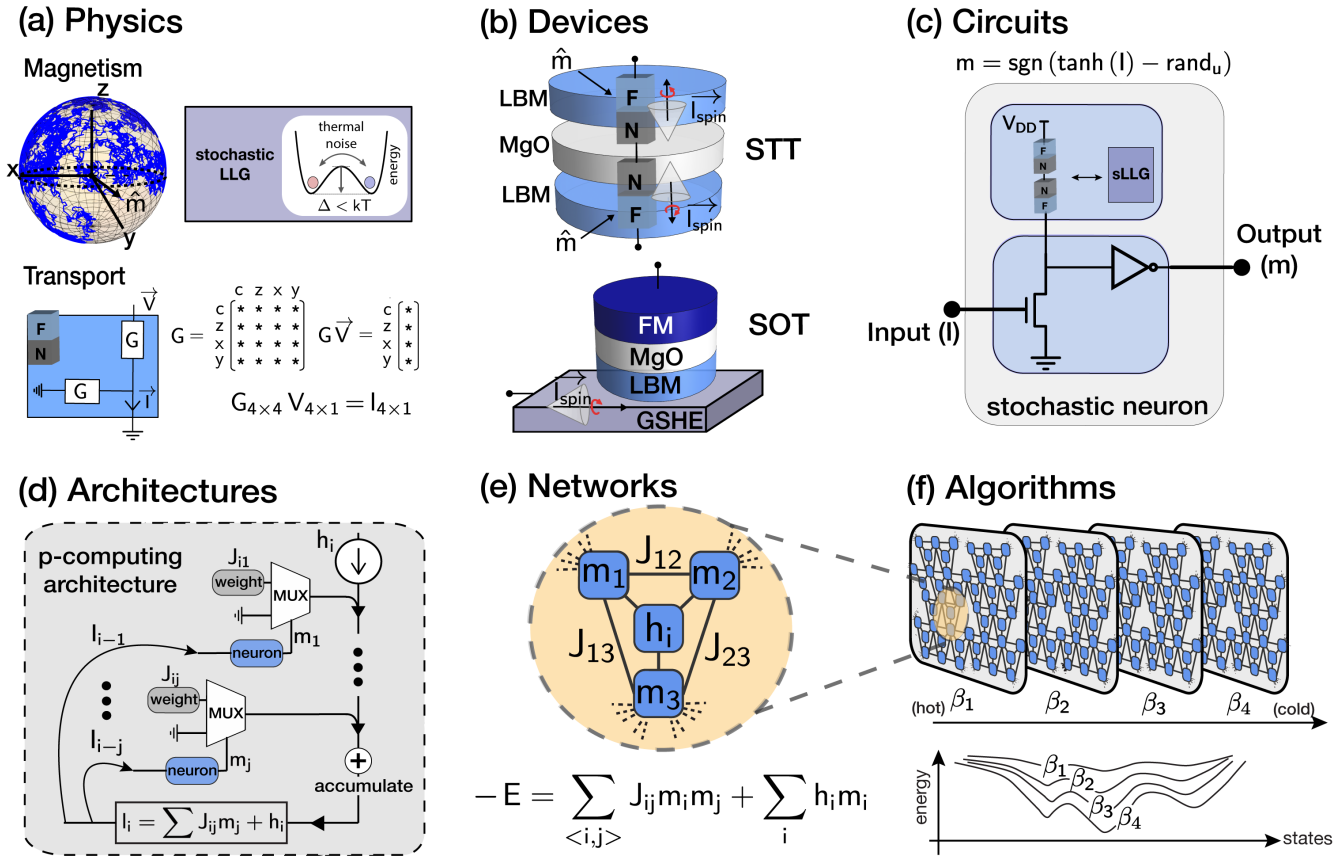


FIG. 1. **Physics to systems perspective with modular spin-circuits** (a) Physics: Spin-circuits solve transport and magnetization dynamics self-consistently. (b) Devices: example stochastic MTJs (with spin-orbit and spin-transfer torque) using low-energy barrier magnets. (c) Circuits: stochastic neurons (p-bits) built out of stochastic MTJs (d) Architectures: Probabilistic architectures with interacting stochastic neurons (e) Networks: networks of p-bits mapped to computationally hard optimization problems (f) Algorithms: powerful algorithms that use replicas of probabilistic networks to help solve these optimization problems.

$I_i(uv^*)$. The 4-component spin-circuit equations have later been converted into convenient and intuitive 4-component circuits where currents and voltages carry 3-spin and 1-charge components that are related by 4×4 conductances matrices. Many examples of spin-circuits to model existing and evaluate new device concepts have been performed over the years, by the authors and others^{12–34}.

We first give a brief introduction to the spin-circuit approach discussing the basics of the transport and magnetism modules and how they interact. To illustrate how extensible and modular the approach is, we present several original examples of the approach by constructing new spin-circuits. Some of our examples are chosen in the context of a new and emerging computational paradigm with probabilistic bits, covering physics, devices, circuits, architectures, networks, reaching all the way up to the algorithms that run on this stack (FIG. 1). The ideas related to probabilistic computing came long after the spin-circuit approach but as we will show, spin-circuits have been instrumental in helping uncover new physics and new potential applications due to their modularity enabling a “plug and play” approach.

II. MODULAR SPIN CIRCUITS

The two main ingredients in the spin-circuit approach are transport and magnetism modules that need to be solved self-consistently. Transport timescales are typically much faster than magnetization dynamics and this allows a lumped circuit description of transport modules that are solved for each new magnetization configuration in the circuit. We first start by describing spin-transport modules.

A. Spin transport with 4-component circuits

Transport modules are naturally represented as circuits but they need to be generalized to include spin transport. The principled way to do this is to start from a quantum transport formulation of the density matrix ρ and turn it into a 4-component vector:

$$\frac{1}{2} \begin{bmatrix} N + S_z & S_x - iS_y \\ S_x + iS_y & N - S_z \end{bmatrix} \rightarrow \begin{bmatrix} N \\ S_z \\ S_x \\ S_y \end{bmatrix}$$

where N , S_z , S_x , S_y represent the charge and spin densities at a physical point in the channel material.

One can then obtain transport equations for these 4-component vectors for coherent³⁵ or incoherent channels (see Chapter 24 in³⁶). After this $\rho \rightarrow V_{4 \times 1}$ transformation, the key quantity that emerges is a 4×4 conductance matrix relating 4-component currents to 4-component voltages. The non-conservative nature of spin-currents is naturally handled by shunt conductances that are connected to grounds. The resulting circuits fully satisfy Kirchhoff's laws and can be handled by powerful circuit simulators^{11,15,37}. A microscopic formulation of 4-component formulation of spin-currents was first explored in Ref.'s^{9,10}, focusing on metallic and ferromagnetic channels. In our view however the spin-circuit formalism is much broader and starting from microscopic theory may not always be necessary or possible, yet, phenomenological 4-component spin-circuit models can still be obtained. Examples of these include spin-circuits for channels with spin-momentum locking³⁸ such as heavy metals with giant spin Hall effect²⁰, topological insulators^{20,23}, magnonic transport magnetic insulators³⁹ and others.

For many spintronic devices, a key component is a ferromagnet-normal metal interface (F|N) where the spin-transfer-torque effect occurs. A four-component circuit formulation of the F|N interface can be obtained from scattering theory or the non-equilibrium Green's function formalism^{9,35,37}. The F|N interface consists of a series and a shunt component (FIG. 2a) that both depend on the orientation of the ferromagnet. When the ferromagnet points in the +z direction, these conductances are given by:

$$G_{se}/G_0 = \begin{array}{c|cccc} & c & z & x & y \\ \hline c & 1 & P & 0 & 0 \\ z & P & 1 & 0 & 0 \\ x & 0 & 0 & 0 & 0 \\ y & 0 & 0 & 0 & 0 \end{array}, G_{sh}/G_0 = \begin{array}{c|cccc} & c & z & x & y \\ \hline c & 0 & 0 & 0 & 0 \\ z & 0 & 0 & 0 & 0 \\ x & 0 & 0 & a & b \\ y & 0 & 0 & -b & a \end{array}$$

where G_0 is the interface conductance, P is the interface polarization, a, b are the real and imaginary coefficients of the "spin-mixing conductance", respectively. The form of these conductances is intuitive: the series conductance creates spin-polarized spin currents when subject to a charge potential and shunt conductances are responsible for absorbing transverse spin currents responsible for the spin-transfer-torque effect.

Naturally, in settings where transient behavior needs to be examined, conductances need to be modified in conjunction with moving ferromagnetic magnetization vectors. This can be carried out by a standard rotation matrix that leaves the charge components (cc) unchanged but modifies spin components. Expressing magnetization in spherical coordinates, an arbitrary magnet direction (θ, ϕ) can be reached via $G_{\{sh,se\}} = [U_R]^T [G_{\{sh,se\}}] [U_R]$, where the rotation matrix $[U_R]$ is given by¹¹:

$$\begin{array}{c|cccc} & c & z & x & y \\ \hline c & 1 & 0 & 0 & 0 \\ z & 0 & \cos \theta & \sin \theta \cos \phi & \sin \theta \sin \phi \\ x & 0 & -\sin \theta \cos \phi & \cos \theta + \sin^2 \phi (1 - \cos \theta) & -\sin \phi \cos \phi (1 - \cos \theta) \\ y & 0 & -\sin \theta \sin \phi & \sin \phi \cos \phi (1 - \cos \theta) & \cos \theta + \cos^2 \phi (1 - \cos \theta) \end{array}$$

In circuit simulators, we first obtain a fully parameterized rotated conductance that receives instantaneous magnetization directions for transient simulations.

As a simple example that demonstrates the modularity of such spin-circuits, FIG.2(a) shows a metallic spin-valve where the relative angle between the ferromagnets is changed. In this case (and in many cases involving spin-circuits) the charge conductance (or the c-c component) of the equivalent conductance can be analytically calculated (see Eq. 124 in⁹ with $a = 2\Re(G_{\uparrow\downarrow}/G_0)$, while the imaginary part b is set to 0, which is typical for metallic interfaces). FIG. 2(a) shows the magnetoresistance effect on the charge conductance where the analytical result is compared to a numerical one obtained from a circuit simulator (HSPICE).

This example shows the magnetoresistive change in the charge conductance, but the spin-circuit also captures important spin current information that can be readily extracted. Technically, what we illustrate here is a metallic spin-valve. Remarkably, *multiplying* two conductance matrices instead of adding them in series seems to capture the non-trivial magnetic tunnel junction physics¹⁹. The intuition behind this is the exponential decay of conductance across two tunneling interfaces in series $G_{eq} \propto G_1 G_2$ which seems to generalize to matrix conductances.

The spin-valve example we show in FIG. 2 may seem elementary however the approach is more general. Recently, Ref.⁴⁰ analyzed a complicated magnetic tunnel junction design with two synthetic antiferromagnetic layers (4 ferromagnets) using the same approach, obtaining results in agreement with experimental features observed in similar systems⁴¹.

B. Magnetization dynamics via Landau-Lifshitz-Gilbert equation

The transport captured by spin-circuits needs to be solved self-consistently with magnetization dynamics. Large ferromagnets in experiments typically contain many domains and to get realistic dynamical behavior, sophisticated "micromagnetics" tools need to be used⁶. These tools solve partial differential equations that are hard to combine with circuit simulators. Our approach is to assume monodomain magnets and use the stochastic Landau-Lifshitz-Gilbert (sLLG) equation to model magnetization dynamics. This approximation gets better as magnets are scaled down to small dimensions but more importantly, it allows magnetism and transport modules to be readily coupled in circuit simulators. Moreover, as we show in Section III, multiple monodomain LLG modules can be combined to describe multi-domain physics of nanomagnets, in principle. The single sLLG model incorporates finite temperature physics, dipolar and exchange coupling and spin-transfer torques.

The sLLG equation is a non-linear 2-dimensional ordinary differential equation where the magnetization evolves on the

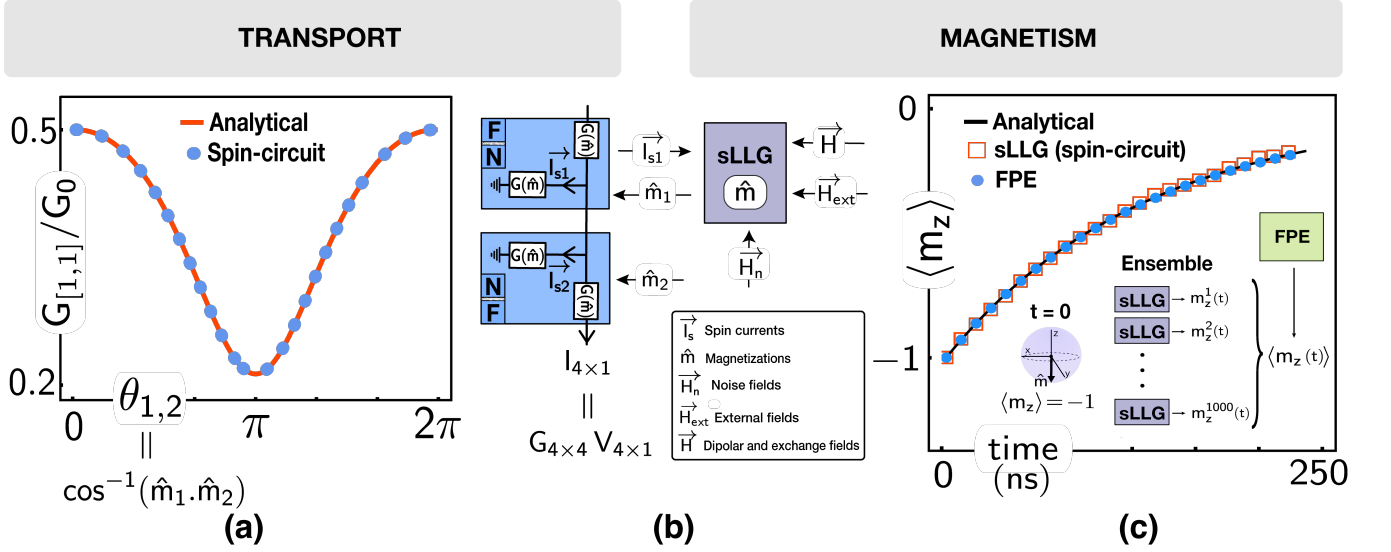


FIG. 2. **Transport and magnetism** (a) An example spin-valve built out of two interfaces is shown. Numerical results obtained from spin-circuits are compared with theory⁹ where the charge conductance shows magnetoresistance as a function of the relative angle between the ferromagnets. (b) Spin-circuit model illustrating the interaction between the magnetization dynamics (modeled by sLLG) and transport modules. The transport model receives two magnetization vectors from the stochastic LLG and produces 4-component spin currents carrying charge and spin information. sLLG receives spin currents and magnetic fields and produces a magnetization vector. (c) sLLG results are benchmarked with the Fokker Planck equation (FPE). 1000 low-barrier nanomagnets (with a very small perpendicular magnetic anisotropy) are prepared in the -1 direction and left to relax. The average magnetization $\langle m_z \rangle$ is measured over time and compared to FPE and the analytical solution (see text).

surface of the unit sphere^{42–46}:

$$(1 + \alpha^2) \frac{d\hat{m}}{dt} = -|\gamma| \hat{m} \times \vec{H} - \alpha |\gamma| \hat{m} \times (\hat{m} \times \vec{H}) + \frac{\alpha}{qN} (\hat{m} \times \vec{I}_s) + \frac{1}{qN} (\hat{m} \times (\vec{I}_s \times \hat{m})) \quad (1)$$

where α is the damping coefficient, q is the electron charge, γ is the electron gyromagnetic ratio, \vec{I}_s is the received spin current. N is the total number of spins in the free layer, $N = M_s \text{Vol.} / \mu_B$, where M_s is the saturation magnetization, μ_B being the Bohr magneton. In addition to all the fields (uniaxial, demagnetization, external magnetic fields, strain-induced anisotropy fields, etc.) that go into the effective field \vec{H} , the effect of thermal noise also enters as a fluctuating magnetic field with the following properties:

$$\text{Var.}(H_n^{x,y,z}) = \frac{2\alpha k_B T}{|\gamma| \mu_0 M_s \text{Vol.}}, \quad \mathbb{E}[H_n^{x,y,z}] = 0 \quad (2)$$

where T is the temperature, k_B is the Boltzmann's constant and μ_0 is free space permeability. The noise is assumed to be independent in all 3-dimensions.

To solve the sLLG equation using powerful circuit simulators, we express the LLG equation in a form of coupled capacitors: $CdV/dt = I$ ^{16,47} where the voltages map to magnetizations and non-linear current sources map to the different terms in the LLG equation. Note that our approach does not use linearization or make any approximation: through the

use of non-linear and state-dependent current sources, the *full* LLG equation is solved in circuit simulators. The numerically challenging transient noise simulations can be handled by reformulating existing noise models that are used for resistor noise in HSPICE⁴⁸.

Solving the stochastic LLG requires care, especially if done in closed-source circuit simulators. The time dependence of noise fields, the choice of convention in integration (Itô vs Stratonovitch), and the way the variance of the noise enters in HSPICE may not be obvious. Our approach to such uncertainties is to rigorously benchmark the sLLG by its corresponding Fokker-Planck equation (FPE)^{44,49,50}. For a magnet with cylindrical symmetry, the time-dependent FPE reads⁴⁴:

$$\frac{\partial \rho(m_z, t)}{\partial \tau} = \frac{\partial}{\partial m_z} \left[(i - h - m_z)(1 - m_z^2) \rho + \frac{1 - m_z^2}{2\Delta} \frac{\partial \rho}{\partial m_z} \right]$$

as long as the external fields h and spin currents i are defined to be in the $\pm z$ direction. τ is the normalized time, $\tau = (1 + \alpha^2) / (\alpha \gamma H_k) / t$, where α is the damping coefficient, H_k is the uniaxial anisotropy constant, γ is the gyromagnetic ratio, and t is the real time. Δ represents the energy barrier of the magnet normalized with $k_B T$.

To benchmark our sLLG solver in HSPICE with FPE, we consider an ensemble of low-barrier nanomagnets all prepared in the $m_z = -1$ direction, which are then left to fluctuate on their own in the absence of any fields and currents. We perform 1000 independent (with identical parameters) sLLG simulations and numerically plot the average m_z component as a

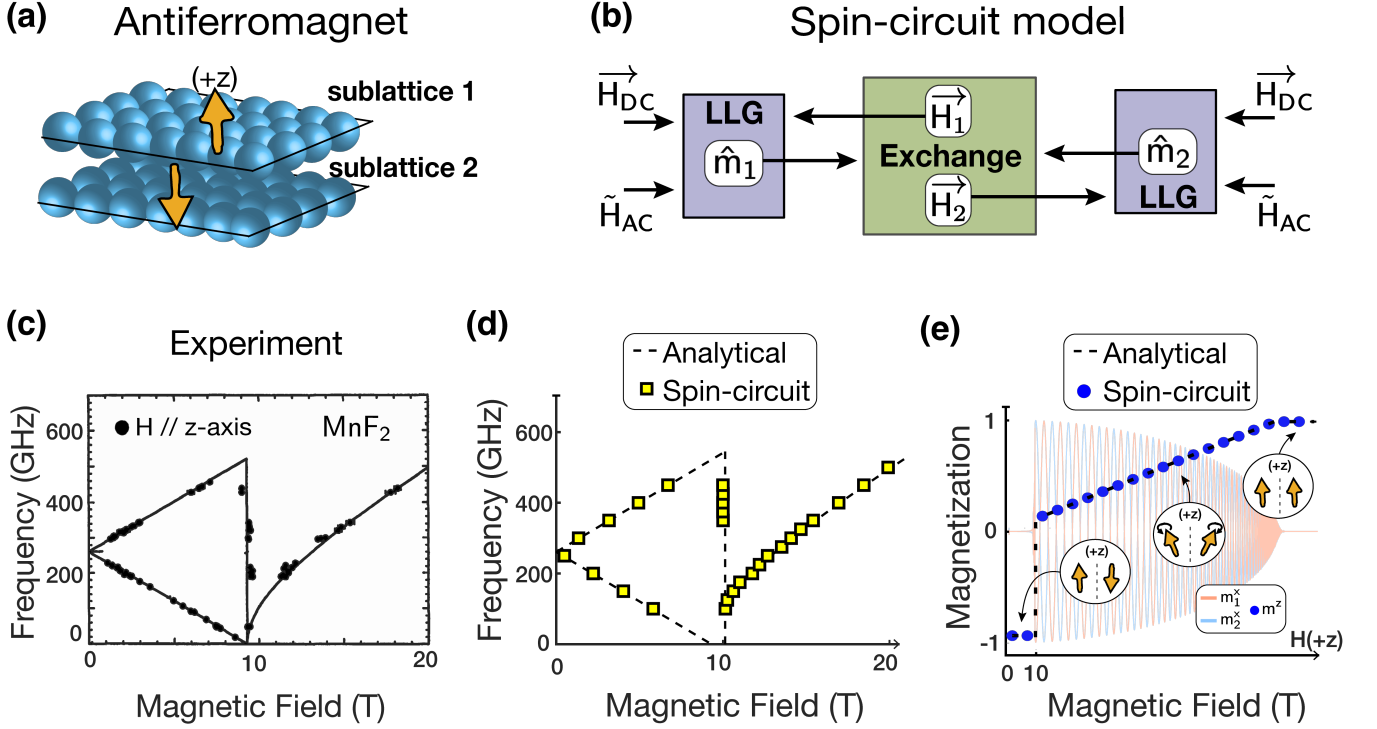


FIG. 3. **Antiferromagnetic resonance (AFMR) with spin-circuits** (a) Sketch of an antiferromagnet where two sublattices with opposing magnetizations. (b) Spin circuit model of the AFM with two antiferromagnetic layers analyzed by two LLGs coupled with exchange interactions. (c) Experimental results for AFMR in MnF_2 ⁵¹. (d) Numerical results obtained from spin-circuits for AFMR, compared to known theory. (e) Easy-axis (z) component of the magnetization vector analysis over an external magnetic field applied in the $+z$ direction. At a critical field, the sublattice spins enter the “spin-flop” region where they both develop a small m_z component in the direction of the magnetic field. In all cases, spin-circuits provide excellent agreement with known theory.

function of time. The same quantity can be obtained from a numerical solution of the FPE, which solves for $\rho(\tau, m_z)$. We then integrate ρ to obtain $\langle m_z(\tau) \rangle = \int \rho(m_z, \tau) dm_z$. The FPE sLLG comparison is shown in FIG. 2c with excellent agreement. Further, both numerical methods can be understood by an analytical expression for the average m_z (following a similar approach in⁵²:

$$C(t) = \exp\left(-2\alpha\gamma\frac{k_B T}{M_s \text{Vol.}}|t|\right) \quad (3)$$

Eq. 3 is also shown as the analytical solution in FIG. 2 in agreement with FPE and sLLG. These simple examples where sLLG is matched with an FPE approach which in turn is matched with analytical expectations to ensure the validity of our numerical solvers.

III. NATURAL ANTIFERROMAGNETS WITH SPIN-CIRCUITS

As mentioned earlier, our approach with magnetization dynamics necessarily assumes the monodomain approximation. Could spin-circuit models be built out of coupled magnetizations? We answer this question in the context of natural anti-

ferromagnets (AFM) by matching the experimental antiferromagnetic resonance behavior observed in MnF_2 ⁵¹. FIG. 3a-b shows the two coupled atomic sublattices and the corresponding spin-circuit model. The exchange fields between two magnets can be obtained from an energy model of the form:⁵⁴

$$E_{ex} = -M_s(\text{Vol}_1 + \text{Vol}_2)(J_{ex})(\hat{m}_1 \cdot \hat{m}_2) \quad (4)$$

where the effective field that enters the LLG becomes:

$$[H_{ex}]_i = -\frac{1}{(M_s)_i V_i} \nabla_{\hat{m}_i}, \quad E_{ex} = J_{ex} \frac{(\text{Vol}_1 + \text{Vol}_2)}{\text{Vol}_i} m_j \quad (5)$$

In the spin-circuit, the exchange fields are assumed to change “instantaneously” for the two coupled LLGs. The tools available to circuit simulators make measuring the AFMR frequency highly convenient. We apply an external DC magnetic field along the z -axis and sweep the frequency of an external AC magnetic field (perpendicular to the z -axis) and measure the transient response of the m_z components of the constituent spins. The frequency of the AC field at which this response is maximum is recorded as the AFM resonance frequency at that DC field. Interestingly, this is not too different from how the AFMR is measured experimentally.

By linearizing the coupled LLG equations, two sets of

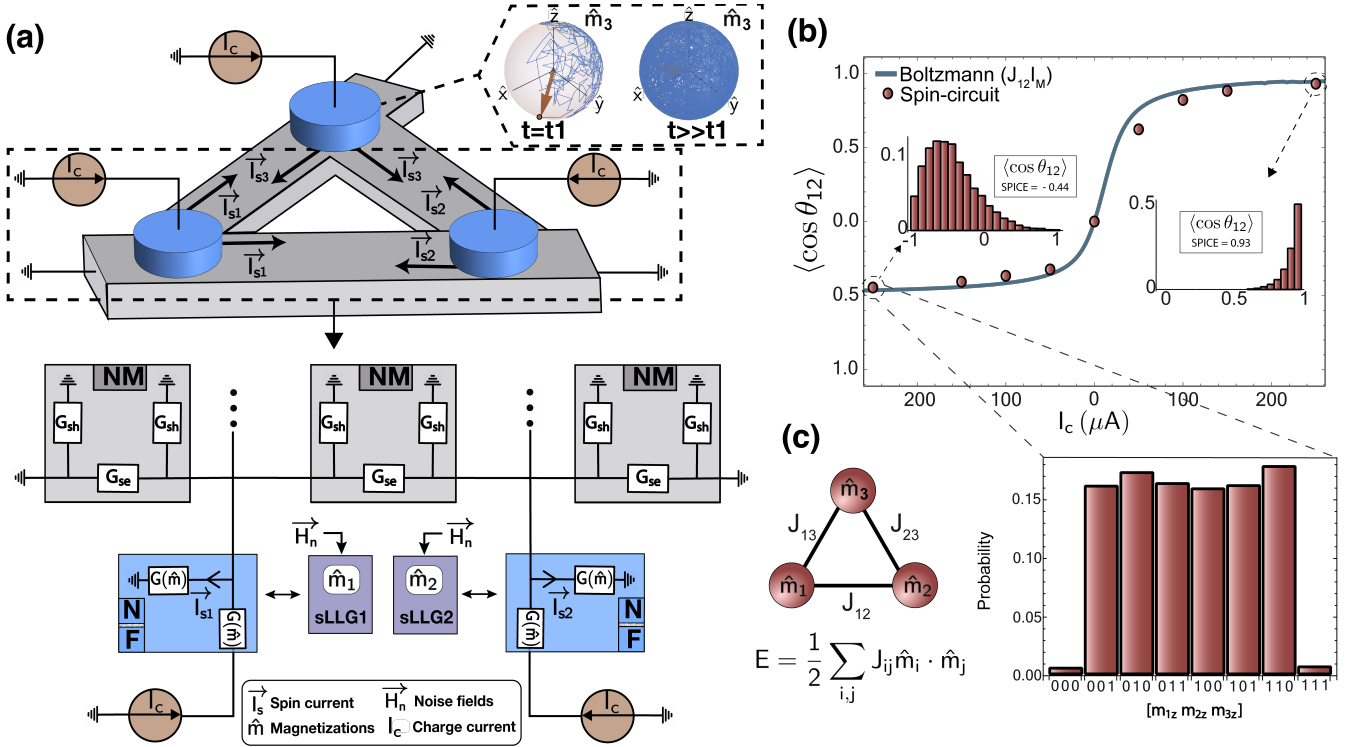


FIG. 4. **Non-local spin valve (NLSV) with low-barrier nanomagnets (LBM)** (a) Physical structure consisting of networks of LBMs. A charge current is injected from LBMs going to a nearby local ground. Spin currents polarized in the direction of fluctuating LBMs are routed to one another. Inset shows an example of how magnetization dynamics \hat{m} evolve over time for an LBM with low perpendicular anisotropy. The bottom panel shows the spin-circuit corresponding to the physical structure. (b) The average of the relative angle between LBM 1 and LBM 2 is measured as a function of injected charge currents, showing ferromagnetic (at positive I_c) and antiferromagnetic (at negative I_c) coupling. The numerical results are compared with those obtained from the Boltzmann law obtained from the Heisenberg Hamiltonian. This correspondence between the unitless Heisenberg Hamiltonian and spin-circuit requires a mapping factor I_M with units of currents (see text and Ref.⁵³). (c) A histogram of three LBMs at large negative currents where for better illustration the magnetizations \hat{m} are binarized by thresholding at $\hat{m}_z = 0$. The system shows frustration in the antiferromagnetic configuration.

AFMR frequencies can be obtained^{55,56}:

$$f_{\text{res}} = \gamma \left(\sqrt{H_K \cdot (H_K + 2 \cdot J_{\text{ex}})} \pm H_{\text{ext}} \right) \quad (6)$$

$$f_{\text{res}}^{\text{sf}} = \gamma \sqrt{H_{\text{ext}}^2 - (2 \cdot J_{\text{ex}} \cdot H_K + H_K^2)} \quad (7)$$

where H_K is the uniaxial anisotropy of individual sublattices, H_{ext} is the external magnetic field and γ is the gyromagnetic ratio for the electron. In FIG. 3c-d, we observe that around 10 T, the coupled AFM spins enter the interesting “spin-flop” region where they each develop a small m_z component and start precessing about this axis (FIG. 3e).

As FIG. 3 shows, all of this physics is captured by the spin-circuit formalism quantitatively. The availability of AC/DC sources, transient and AC simulation options offer a convenient platform to study magnetization physics in a modular manner. The ability to combine such magnetic models with materials and transistors makes the spin-circuit approach appealing.

IV. ENGINEERED ANTIFERROMAGNETS WITH NON-LOCAL SPIN VALVES

Next, we show an example non-local spin valve (NLSV) setup that couples low-barrier nanomagnets (LBMs) to engineer a “Heisenberg machine” using spin-circuit models. The setup we consider here has recently been proposed theoretically⁵³ and to the best of our knowledge no experiments involving LBMs and NLSVs have yet been performed. Our main point is that modular spin-circuits can be useful to motivate new experiments, provide quantitative insights into new physics and estimate energy and delay metrics before the physical realization of a proposed system.

In previous sections, we described how we can model magnets by coupling the transport model (FIIN) with the magnetism model (LLG). For channel materials used in NLSVs, we also introduce the Normal Metal (NM) model, which we use to describe the physical connection between the magnets. The NM model consist of a π -network with two shunt conductance G_{sh} separated by a series conductance G_{se} as shown in FIG. 4¹³:

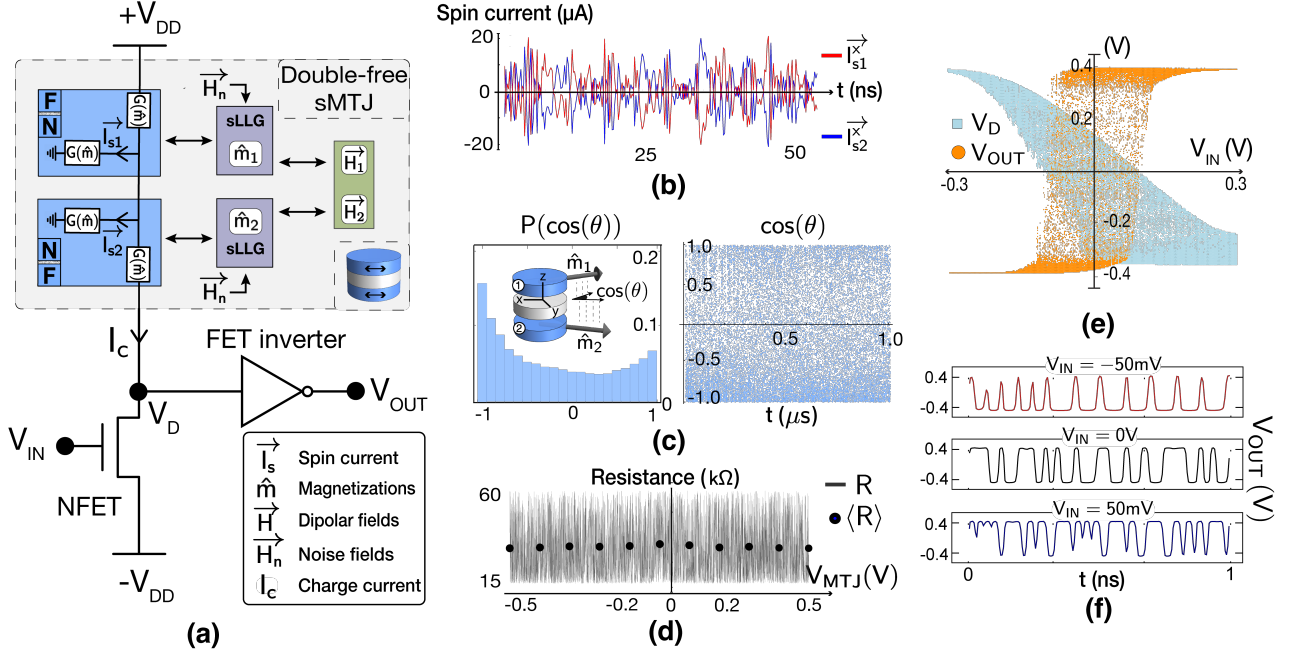


FIG. 5. **Probabilistic bit with double-free-layer stochastic MTJs** (a) Self-consistent magnet and transport model combined with transistors to model a probabilistic bit. (b) Time-dependent spin currents are produced from the transport model that goes into the sLLG modules. We show the x -component of spin-currents for magnets, 1 and 2. (c) Histogram and time fluctuations for the $\cos(\theta)$ between m_z components of magnet 1,2 for the double-free-layer sMTJ. Slight anti-parallel tendency is due to the dipolar coupling which is not completely overcome by thermal fields. (d) Resistance of the sMTJ is measured while the voltage is swept from -0.5 to 0.5 V over 1 ms. The discrete data points are average resistances over 500 ns showing the roughly bias-independent characteristics of the device. (e) The drain node (V_D) and the output of the inverter (V_{OUT}) are measured while the input (V_{IN}) is swept from -0.3 V to 0.3 V over 1 ms. The output of the inverter shows the binary stochastic neuron behavior. (f) Digital output fluctuations over time for the probabilistic bit output at different bias conditions for V_{IN} .

$$G_{se} = \begin{bmatrix} c & z & x & y \\ c & G_c & 0 & 0 & 0 \\ z & 0 & G_s & 0 & 0 \\ x & 0 & 0 & G_s & 0 \\ y & 0 & 0 & 0 & G_s \end{bmatrix}, \quad G_{sh} = \begin{bmatrix} c & z & x & y \\ c & 0 & 0 & 0 & 0 \\ z & 0 & G'_s & 0 & 0 \\ x & 0 & 0 & G'_s & 0 \\ y & 0 & 0 & 0 & G'_s \end{bmatrix}$$

where $G_c = A_{NM}/(\rho_{NM}L)$, $G_s = A_{NM}/(\rho_{NM}\lambda_s)\text{csch}(L/\lambda_s)$, and $G'_s = A_{NM}/(\rho_{NM}\lambda_s)\tanh(L/2\lambda_s)$. A_{NM} denotes the area, ρ_{NM} is the NM resistivity, L is the length, and λ_s is the spin-diffusion length. These matrices are obtained from microscopic spin-diffusion equations, accounting for the non-conservative nature of spin currents through the shunts.

In this example, we stick to spin-isotropic channels without any spin-momentum locking, however, experiments with heavy metals that exhibit Giant Spin Hall Effect⁵⁷ have been successfully modeled with spin circuits^{11,20}.

The basic idea of the coupled NLSVs in FIG. 4a is to engineer a system of LBMs that interact via pure spin currents. To achieve this, a charge current passes through each magnet with a nearby ground. Then, spin-currents polarized in the instantaneous direction of the magnetization of the LBMs are sent toward neighboring LBMs. The key point is to design a system that takes samples from the classical Heisenberg model:

$$E = -\frac{1}{2} \sum_{i,j} J_{ij} (\hat{m}_i \cdot \hat{m}_j) \quad (8)$$

where J_{ij} are the interaction terms and m_i are 3D-magnetization vectors. Finding low-energy (or equilibrium) states of the Heisenberg Hamiltonian for probabilities p_i ($\propto \exp(-E/kT)$) is computationally challenging. As such, engineering a system of LBMs to sample from the classical Heisenberg model can be useful for optimization and/or sampling problems. The read-out mechanisms or practical applications of this system is beyond the scope of our discussion here and can be found in Ref.⁵³.

From a modeling perspective, the system shown in FIG. 4a is quite challenging: one needs to model the NLSV transport where charge and spin-currents are modeled properly. Moreover, a self-consistent solution of stochastic LLG equations with transport modules is needed. In the presence of incoming spin-currents that are transport-dependent, the sLLG equations provide magnetization vectors that control the interface conductances. The spin-circuit approach allows a seamless implementation of this highly complicated physical system. As shown in FIG. 4, the magnitude and the sign of the injected charge current control the degree of correlation between two magnets (1 and 2). When the injected charge currents are negative, the coupling between the three LBMs exhibits antiferromagnetic coupling as shown in FIG. 4c, as would be expected from the engineered interactions obtained from a Heisenberg model with negative couplings.

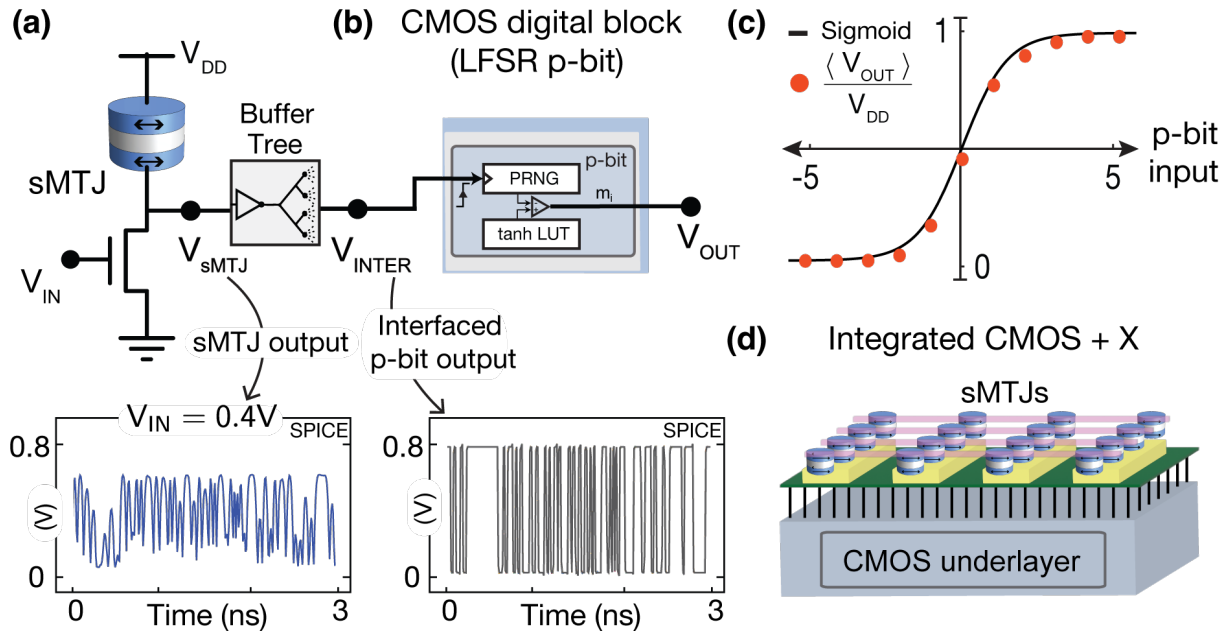


FIG. 6. **CMOS + X (stochastic MTJ) platforms** (a) An sMTJ-based binary stochastic neuron (p-bit) is interfaced with a digital CMOS-based circuit to trigger a digital p-bit emulator. The bottom panel shows SPICE results for the analog fluctuations at the drain (V_{SMTJ}) of the NMOS transistor. (b) Rail-to-rail stochastic fluctuations obtained after a buffer tree (V_{INTER}) is inserted between the single sMTJ-based p-bit and the large digital CMOS block. CMOS block contains a low-quality and inexpensive pseudo-random number generator (PRNG) along with a look-up table to obtain tunability. This hybrid setup with the sMTJ circuit increases the quality of randomness that can be obtained from the digital p-bit block alone (see Ref.⁵⁸) (c) Tunability of the heterogeneous structure as a probabilistic bit is shown with time-averaged V_{OUT} over 1000 ns in SPICE. (d) In the future, millions of sMTJs can provide nearly-free true randomness to CMOS underlayers for various probabilistic computing applications.

V. FUNCTIONAL SPIN-CIRCUITS WITH TRANSISTORS

So far, the spin-circuit examples we considered have been based on spintronic building blocks with increasing sophistication, albeit without the use of any transistors. An emerging trend in the field in the beyond Moore era of electronics is the notion of *domain-specific* computation where conventional complementary metal-oxide semiconductor (CMOS) transistors are augmented with emerging technologies (X) to create CMOS+X systems, where X can stand for anything from spintronics, photonics, memristors, superconducting circuits, and others.

FIG. 5 shows how a new type of stochastic magnetic tunnel junction can readily be modeled and analyzed using the spin-circuit approach, in conjunction with state-of-the-art transistor models. Typically, magnetic tunnel junctions employ a fixed layer such that the resistance of the junction correlates with the magnetization of a free layer. With the emergence of probabilistic computing⁵⁹ and the need for fast, energy-efficient, and scalable random number generators, a recent approach has been to design sMTJs with no fixed layers^{40,60,61}.

Typically, physics-based device models cannot easily be interfaced with transistor models, whereas the SPICE formulation of spin-circuits allows seamless integration with CMOS. FIG. 5 shows such a combination where a spin-valve made out of two LBMs is connected to an n-MOS transistor. Here, we use FinFET models from the open-source predictive technology models (PTM)⁶², in principle, however, any other FET

model could be combined with spin-circuits. When we combine spin-circuits that carry 4-component currents and voltages with ordinary circuits that only carry charge currents, we only attach the charge current terminals to each other, since any other spin information can be ignored in extended charge circuits. The double-free layer sMTJ exhibits an interesting voltage-independent resistance profile⁶³. This behavior is reproduced by the spin-circuit model where the two symmetric layers receive spin-currents with opposing signs (FIG. 5b), leading to nearly uniform fluctuations (FIG. 5c) and weak voltage-bias dependence (FIG. 5d). The slight asymmetry favoring an anti-parallel configuration stems from the dipolar coupling between the easy-plane magnets which is included in the spin-circuit simulation (following the methodology in Ref.⁶⁰).

Finally, FIG. 5e-f shows the full input-output characteristics of what has been called a probabilistic or p-bit⁶⁴ that is obtained from our full model. The combination of magnetization dynamics, dipolar and thermal noise fields, 4-component interface conductances, and transistors in a sound powerful circuit simulator shows the power and flexibility of the spin-circuit approach.

VI. FROM SPIN-CIRCUITS TO SYSTEMS

So far, the spin-circuit examples we illustrated are all at the device or the circuit level. The combination of spin-circuits with transistors unlocks a much larger space of possibilities.

As a final example, we describe a hybrid system where a true random number generator (TRNG) augments a low-quality pseudo-random number generator (PRNG) (even though our modeling in SPICE will use PRNGs for the sMTJ part of this circuit, the RNG quality used for this purpose will be much higher than that of an LFSR without noticeable differences between an actual MTJ, see Ref.⁵⁸ for details). FIG. 6 shows the p-bit circuit from FIG. 5 “clocking” a digital p-bit (FIG. 6a-b) to generate a tunably random behavior (whose average is shown in FIG. 6c).

The motivation is to increase the quality of randomness that is extracted from inexpensive linear feedback shift register (LFSR)-based PRNG by clocking the PRNG with random arrivals of sMTJ fluctuations. This setup was realized using physical sMTJs in a recent experiment that established the concept⁵⁸. Considering the expensive nature of PRNGs, augmenting them with the true randomness of millions of sMTJs in integrated CMOS + X systems (FIG. 6d) seems desirable.

The CMOS block consists of a PRNG and a lookup table (LUT) for the hyperbolic tangent function consisting of thousands of transistors. The CMOS design is synthesized from the open-source ASAP7 Predictive PDK⁶⁵ and the details of how this synthesis is performed can be found in Ref.⁵⁸.

The bottom panels of FIG. 6 show simulations obtained from this hybrid circuit where a single sMTJ-based circuit drives thousands of transistors. An important detail, immediately captured by the spin-circuit approach is that of loading. Without a “buffer tree” where several stages of inverters distribute the capacitive load of the CMOS p-bit that is seen by the single sMTJ-based circuit, the clocking does not work. These nontrivial loading effects at the interfaces of physics-based and digital systems are naturally captured by the powerful spin-circuit approach that is otherwise easy to miss. In addition to loading, key circuit and system metrics such as energy-delay can be reliably calculated for many types of exploratory systems.

VII. CONCLUSION

We have described the spin-circuit approach connecting the microscopic physics of spins and magnets all the way up to circuits and systems. We believe that such a physics-based, modular, CMOS-compatible modeling approach will be critical in evaluating and exploring new hardware systems in the beyond-Moore era of electronics. Despite the wide focus of this paper, there are many other spintronic phenomena that have been modeled by spin-circuits and we did not get into these, e.g. full compute life-cycle modeling of skyrmions and domain walls⁶⁶. Beyond spins, a similar circuit framework for new and emerging phenomena can be constructed. Extensions may include pseudospins, valley currents³⁰, superconductivity, photonics, and qubit systems⁶⁷, all within the context of powerful, industry-standard transistor-compatible circuit simulators. These extended spin-circuits could enable a rapid and robust evaluation of CMOS+X systems of the future.

CODE AND DATA AVAILABILITY

All the codes used in this study are publicly available in the Github repository [<https://github.com/OPUSLab/Spin-Circuit-Designs>].

ACKNOWLEDGMENTS

We acknowledge the U.S. National Science Foundation (NSF) support through CCF 2106260, through a CAREER award, SAMSUNG Global Research Outreach (GRO) grant. We also acknowledge support from ONR-MURI grant N000142312708, OptNet: Optimization with p-Bit Networks. Use was made of computational facilities purchased with funds from the National Science Foundation (CNS-1725797) and administered by the Center for Scientific Computing (CSC). The CSC is supported by the California NanoSystems Institute and the Materials Research Science and Engineering Center (MRSEC; NSF DMR 2308708) at UC Santa Barbara.

AUTHOR CONTRIBUTIONS

KYC and SD wrote the initial draft of the manuscript. KS, SB, NSS have designed the spin-circuits, obtained results, drew the figures and prepared open-source models. All authors have provided feedback and helped improve the manuscript.

COMPETING INTERESTS

All authors declare no financial or non-financial competing interests.

¹William J Dally, Yatish Turakhia, and Song Han. Domain-specific hardware accelerators. *Communications of the ACM*, 63(7):48–57, 2020.

²Giovanni Finocchio, Jean Anne Currihan Incorvia, Joseph S Friedman, Qu Yang, Anna Giordano, Julie Grollier, Hyunsoo Yang, Florin Ciubotaru, Andrii Chumak, Azad Naeemi, et al. Roadmap for unconventional computing with nanotechnology. *Nano Futures*, 2023.

³nanohub.org. Modular approach to spintronics. <https://nanohub.org/groups/spintronics>.

⁴Shehrin Sayed, Kerem Y Camsari, Rafatul Faria, and Supriyo Datta. Rectification in spin-orbit materials using low-energy-barrier magnets. *Physical Review Applied*, 11(5):054063, 2019.

⁵Shehrin Sayed, Sayeef Salahuddin, and Eli Yablonovitch. Spin-orbit torque rectifier for weak rf energy harvesting. *Applied Physics Letters*, 118(5), 2021.

⁶Arne Vansteenkiste, Jonathan Leliaert, Mykola Dvornik, Mathias Helsen, Felipe Garcia-Sanchez, and Bartel Van Waeyenberge. The design and verification of mumax3. *AIP advances*, 4(10), 2014.

⁷Jakub Mojsiejuk, Sławomir Ziętek, Krzysztof Grochot, Witold Skowroński, and Tomasz Stobiecki. cmtj: Simulation package for analysis of multilayer spintronic devices. *npj Computational Materials*, 9(1):54, 2023.

⁸T Valet and AJPRB Fert. Theory of the perpendicular magnetoresistance in magnetic multilayers. *Physical Review B*, 48(10):7099, 1993.

⁹Arne Brataas, Gerrit E.W. Bauer, and Paul J. Kelly. Non-collinear magnetoelectronics. *Physics Reports*, 427(4):157–255, 2006.

¹⁰Gerrit E.W. Bauer, Yaroslav Tserkovnyak, Daniel Huertas-Hernando, and Arne Brataas. *From Digital to Analogue Magnetoelectronics: Theory of Transport in Non-collinear Magnetic Nanostructures*, pages 383–396.

- Springer Berlin Heidelberg, Berlin, Heidelberg, 2003. ISBN 978-3-540-44838-9. doi:10.1007/978-3-540-44838-9_27. URL https://doi.org/10.1007/978-3-540-44838-9_27.
- ¹¹Kerem Yunus Camsari. *Modular approach to spintronics*. PhD thesis, Purdue University, 2015.
 - ¹²Srikant Srinivasan, Angik Sarkar, Behtash Behin-Aein, and Supriyo Datta. All-spin logic device with inbuilt nonreciprocity. *IEEE Transactions on Magnetics*, 47(10):4026–4032, 2011.
 - ¹³Srikant Srinivasan, Vinh Diep, Behtash Behin-Aein, Angik Sarkar, and Supriyo Datta. *Modeling Multi-Magnet Networks Interacting via Spin Currents*, pages 1–49. Springer Netherlands, Dordrecht, 2014. ISBN 978-94-007-7604-3.
 - ¹⁴Sasikanth Manipatruni, Dmitri E Nikonov, and Ian A Young. Vector spin modeling for magnetic tunnel junctions with voltage dependent effects. *Journal of Applied Physics*, 115(17), 2014.
 - ¹⁵Sasikanth Manipatruni, Dmitri E Nikonov, and Ian A Young. Modeling and design of spintronic integrated circuits. *IEEE Transactions on Circuits and Systems I: Regular Papers*, 59(12):2801–2814, 2012.
 - ¹⁶Kerem Yunus Camsari, Samiran Ganguly, and Supriyo Datta. Modular approach to spintronics. *Scientific reports*, 5(1):10571, 2015.
 - ¹⁷Kerem Y Camsari, Samiran Ganguly, and Deepanjan Datta. A modular spin-circuit model for magnetic tunnel junction devices. In *2016 74th Annual Device Research Conference (DRC)*, pages 1–2. IEEE, 2016.
 - ¹⁸Qiuyang Li, Penghe Zhang, Haotian Li, Lina Chen, Kaiyuan Zhou, Chunjie Yan, Liyuan Li, Yongbing Xu, Weixin Zhang, Bo Liu, et al. Experiments and spice simulations of double mgo-based perpendicular magnetic tunnel junction. *Chinese Physics B*, 30(4):047504, 2021.
 - ¹⁹Kerem Yunus Camsari, Samiran Ganguly, Deepanjan Datta, and Supriyo Datta. Physics-based factorization of magnetic tunnel junctions for modeling and circuit simulation. In *2014 IEEE International Electron Devices Meeting*, pages 35–6. IEEE, 2014.
 - ²⁰Seokmin Hong, Shehrin Sayed, and Supriyo Datta. Spin circuit representation for the spin hall effect. *IEEE Transactions on Nanotechnology*, 15(2): 225–236, 2016.
 - ²¹Shehrin Sayed, Seokmin Hong, and Supriyo Datta. Multi-terminal spin valve on channels with spin-momentum locking. *Scientific reports*, 6(1): 35658, 2016.
 - ²²Shehrin Sayed, Seokmin Hong, Ernesto E Marinero, and Supriyo Datta. Proposal of a single nano-magnet memory device. *IEEE Electron Device Letters*, 38(12):1665–1668, 2017.
 - ²³Shehrin Sayed, Seokmin Hong, and Supriyo Datta. Transmission-line model for materials with spin-momentum locking. *Physical Review Applied*, 10(5):054044, 2018.
 - ²⁴Jiaxi Hu, David A Deen, and Steven J Koester. Ac small-signal model for magnetoresistive lateral spin valves. *IEEE Transactions on Magnetics*, 55(3):1–8, 2018.
 - ²⁵Ramtin Zand, Arman Roohi, and Ronald F DeMara. Energy-efficient and process-variation-resilient write circuit schemes for spin hall effect mram device. *IEEE Transactions on Very Large Scale Integration (VLSI) Systems*, 25(9):2394–2401, 2017.
 - ²⁶Kuntal Roy. Spin-circuit representation of spin pumping. *Physical Review Applied*, 8(1):011001, 2017.
 - ²⁷Anirudh Iyengar, Swaroop Ghosh, and Srikant Srinivasan. Retention testing methodology for stram. *IEEE Design & Test*, 33(5):7–15, 2016.
 - ²⁸Kerem Y Camsari, Rafatul Faria, Orchi Hassan, Brian M Sutton, and Supriyo Datta. Equivalent circuit for magnetoelectric read and write operations. *Physical Review Applied*, 9(4):044020, 2018.
 - ²⁹Kuntal Roy. Spin-circuit representation of spin-torque ferromagnetic resonance. *IEEE Magnetics Letters*, 12:1–5, 2021.
 - ³⁰Terry YT Hung, Kerem Y Camsari, Shengjiao Zhang, Pramey Upadhyaya, and Zhihong Chen. Direct observation of valley-coupled topological current in mos2. *Science advances*, 5(4):eaau6478, 2019.
 - ³¹Gerard Joseph Lim, Daniel Chua, Weiliang Gan, Chandrasekhar Murapaka, and Wen Siang Lew. Programmable spin-orbit-torque logic device with integrated bipolar bias field for chirality control. *Advanced Electronic Materials*, 6(4):1901090, 2020.
 - ³²Hai Li, Dmitri E Nikonov, Chia-Ching Lin, Kerem Camsari, Yu-Ching Liao, Chia-Sheng Hsu, Azad Naeemi, and Ian A Young. Physics-based models for magneto-electric spin-orbit logic circuits. *IEEE Journal on Exploratory Solid-State Computational Devices and Circuits*, 8(1):10–18, 2022.
 - ³³Sandee Krishna Thirumala, Yi-Tse Hung, Shubham Jain, Arnab Raha, Niharika Thakuria, Vijay Raghunathan, Anand Raghunathan, Zhihong Chen, and Sumeet Gupta. Valley-coupled-spintronic non-volatile memories with compute-in-memory support. *IEEE Transactions on Nanotechnology*, 19: 635–647, 2020.
 - ³⁴Karam Cho, Xiangkai Liu, Zhihong Chen, and Sumeet Kumar Gupta. Utilizing valley-spin hall effect in monolayer wse 2 for designing low power nonvolatile spintronic devices and flip-flops. *IEEE Transactions on Electron Devices*, 69(4):1667–1676, 2021.
 - ³⁵Kerem Y Camsari, Samiran Ganguly, Deepanjan Datta, and Supriyo Datta. Non-equilibrium green’s function based circuit models for coherent spin devices. *IEEE Transactions on Nanotechnology*, 18:858–865, 2019.
 - ³⁶Supriyo Datta. *Lessons from Nanoelectronics: A New Perspective on Transport—Part B: Quantum Transport*. World Scientific, 2018.
 - ³⁷Gopalakrishnan Srinivasan, Abhronil Sengupta, and Kaushik Roy. Magnetic tunnel junction based long-term short-term stochastic synapse for a spiking neural network with on-chip stdp learning. *Scientific reports*, 6: 29545, 2016.
 - ³⁸Shehrin Sayed, Seokmin Hong, Xiaoxi Huang, Lucas Caretta, Arnoud S Everhardt, Ramamoorthy Ramesh, Sayeef Salahuddin, and Supriyo Datta. Unified framework for charge-spin interconversion in spin-orbit materials. *Physical Review Applied*, 15(5):054004, 2021.
 - ³⁹Shehrin Sayed, Vinh Q Diep, Kerem Yunus Camsari, and Supriyo Datta. Spin funneling for enhanced spin injection into ferromagnets. *Scientific reports*, 6(1):28868, 2016.
 - ⁴⁰Kemal Selcuk, Shun Kanai, Rikuto Ota, Hideo Ohno, Shunsuke Fukami, and Kerem Y Camsari. Double-free-layer stochastic magnetic tunnel junctions with synthetic antiferromagnets. *arXiv preprint arXiv:2311.06642*, 2023.
 - ⁴¹Jonathan Z Sun, Christopher Safranski, Philip Trouilloud, Christopher D’Emic, Pouya Hashemi, and Guohan Hu. Easy-plane dominant stochastic magnetic tunnel junction with synthetic antiferromagnetic layers. *Physical Review B*, 108(6):064418, 2023.
 - ⁴²Jonathan Z Sun, TS Kuan, JA Katine, and Roger H Koch. Spin angular momentum transfer in a current-perpendicular spin-valve nanomagnet. In *Quantum Sensing and Nanophotonic Devices*, volume 5359, pages 445–456. International Society for Optics and Photonics, 2004.
 - ⁴³Jonathan Z Sun. Spin-current interaction with a monodomain magnetic body: A model study. *Physical Review B*, 62(1):570, 2000.
 - ⁴⁴William H Butler, Tim Mewes, Claudia KA Mewes, PB Visscher, William H Rippard, Stephen E Russek, and Ranko Heindl. Switching distributions for perpendicular spin-torque devices within the macrospin approximation. *IEEE Transactions on Magnetics*, 48(12):4684–4700, 2012.
 - ⁴⁵L Lopez-Diaz, L Torres, and E Moro. Transition from ferromagnetism to superparamagnetism on the nanosecond time scale. *Physical Review B*, 65(22):224406, 2002.
 - ⁴⁶Sebastian Ament, Nikhil Rangarajan, Arun Parthasarathy, and Shaloo Rakheja. Solving the stochastic landau-lifshitz-gilbert-slonezewski equation for monodomain nanomagnets : A survey and analysis of numerical techniques, 2017.
 - ⁴⁷Georgios D Panagopoulos, Charles Augustine, and Kaushik Roy. Physics-based spice-compatible compact model for simulating hybrid mtj/cmos circuits. *IEEE Transactions on Electron Devices*, 60(9):2808–2814, 2013.
 - ⁴⁸Mustafa Mert Torunbalci, Pramey Upadhyaya, Sunil A Bhave, and Kerem Y Camsari. Modular compact modeling of mtj devices. *IEEE Transactions on Electron Devices*, 65(10):4628–4634, 2018.
 - ⁴⁹Z Li and Shufeng Zhang. Thermally assisted magnetization reversal in the presence of a spin-transfer torque. *Physical Review B*, 69(13):134416, 2004.
 - ⁵⁰Yunkun Xie, Behtash Behin-Aein, and Avik W Ghosh. Fokker—planck study of parameter dependence on write error slope in spin-torque switching. *IEEE Transactions on Electron Devices*, 64(1):319–324, 2016.
 - ⁵¹M. Hagiwara, K. Katsumata, H. Yamaguchi, M. Tokunaga, I. Yamada, M. Gross, and P. Goy. A complete frequency-field chart for the antiferromagnetic resonance in mnm2. *International Journal of Infrared and Millimeter Waves*, 20(4):617–622, 4 1999. ISSN 1572-9559. doi:10.1023/A:1022692506405. URL <https://doi.org/10.1023/A:1022692506405>.

- ⁵²Orchi Hassan, Rafatul Faria, Kerem Yunus Camsari, Jonathan Z Sun, and Supriyo Datta. Low-barrier magnet design for efficient hardware binary stochastic neurons. *IEEE Magnetics Letters*, 10:1–5, 2019.
- ⁵³Saleh Bunaiyan, Supriyo Datta, and Kerem Y. Camsari. Heisenberg machines with programmable spin-circuits, 2023.
- ⁵⁴Randall H Victora and Xiao Shen. Composite media for perpendicular magnetic recording. *IEEE Transactions on Magnetics*, 41(2):537–542, 2005.
- ⁵⁵F. Keffer and C. Kittel. Theory of antiferromagnetic resonance. *Phys. Rev.*, 85:329–337, Jan 1952. doi:10.1103/PhysRev.85.329. URL <https://link.aps.org/doi/10.1103/PhysRev.85.329>.
- ⁵⁶Sergio M. Rezende, Antonio Azevedo, and Roberto L. Rodríguez-Suárez. Introduction to antiferromagnetic magnons. *Journal of Applied Physics*, 126(15):151101, 10 2019. ISSN 0021-8979. doi:10.1063/1.5109132. URL <https://doi.org/10.1063/1.5109132>.
- ⁵⁷Y Niimi, Y Kawanishi, DH Wei, C Deranlot, HX Yang, Mairbek Chshiev, T Valet, A Fert, and Y Otani. Giant spin hall effect induced by skew scattering from bismuth impurities inside thin film cubi alloys. *Physical review letters*, 109(15):156602, 2012.
- ⁵⁸Nihal Sanjay Singh, Keito Kobayashi, Qixuan Cao, Kemal Selcuk, Tianrui Hu, Shaila Niazi, Navid Anjum Aadit, Shun Kanai, Hideo Ohno, Shunsuke Fukami, and Kerem Y. Camsari. Cmos plus stochastic nanomagnets enabling heterogeneous computers for probabilistic inference and learning. *Nature Communications*, 15(1), 2024. ISSN 2041-1723.
- ⁵⁹Shuvro Chowdhury, Andrea Grimaldi, Navid Anjum Aadit, Shaila Niazi, Masoud Mohseni, Shun Kanai, Hideo Ohno, Shunsuke Fukami, Luke Theogarajan, Giovanni Finocchio, Supriyo Datta, and Kerem Y. Camsari. A full-stack view of probabilistic computing with p-bits: Devices, architectures, and algorithms. *IEEE Journal on Exploratory Solid-State Computational Devices and Circuits*, 9(1):1–11, 2023.
- ⁶⁰Kerem Y Camsari, Mustafa Mert Torunbalci, William A Borders, Hideo Ohno, and Shunsuke Fukami. Double-free-layer magnetic tunnel junctions for probabilistic bits. *Physical Review Applied*, 15(4):044049, 2021.
- ⁶¹Jonathan Z. Sun, Christopher Safranski, Philip Trouilloud, Christopher D’Emic, Pouya Hashemi, and Guohan Hu. Easy-plane dominant stochastic magnetic tunnel junction with synthetic antiferromagnetic layers. *Phys. Rev. B*, 108:064418, 2023.
- ⁶²Wei Zhao and Yu Cao. Predictive technology model for nano-cmos design exploration. *ACM Journal on Emerging Technologies in Computing Systems (JETC)*, 3(1):1–es, 2007.
- ⁶³Rikuto Ota, Keito Kobayashi, Keisuke Hayakawa, Shun Kanai, Kerem Y. Camsari, Hideo Ohno, and Shunsuke Fukami. Voltage-insensitive stochastic magnetic tunnel junctions with double free layers. unpublished.
- ⁶⁴Kerem Yunus Camsari, Sayeef Salahuddin, and Supriyo Datta. Implementing p-bits with embedded mtj. *IEEE Electron Device Letters*, 38(12):1767–1770, 2017.
- ⁶⁵Lawrence T. Clark, Vinay Vashishtha, Lucian Shifren, Aditya Gujja, Saurabh Sinha, Brian Cline, Chandarasekaran Ramamurthy, and Greg Yeric. Asap7: A 7-nm finfet predictive process design kit. *Microelectronics Journal*, 53:105–115, 2016. ISSN 0026-2692. doi:<https://doi.org/10.1016/j.mejo.2016.04.006>. URL <https://www.sciencedirect.com/science/article/pii/S002626921630026X>.
- ⁶⁶Mohammad Nazmus Sakib, Hamed Vakili, Samiran Ganguly, Mircea Stan, and Avik W. Ghosh. Compact spice model of topological textures on magnetic racetracks for design space exploration. *2021 International Conference on Simulation of Semiconductor Processes and Devices (SISPAD)*, 2021.
- ⁶⁷Samiran Ganguly, Kerem Y. Camsari, Avik W. Ghosh, and Nibir K. Dhar. Circuits and systems modeling of quantum systems in SPICE. *SPIE DCS: Quantum Information Science, Sensing, and Computation XV*, 12517:1251708, 2023.